ORGAN TOXICITY AND MECHANISMS

Neutralization of interleukin-1 beta attenuates silica-induced lung inflammation and fibrosis in C57BL/6 mice

**Jiali Guo · Nali Gu · Jie Chen · Tingming Shi ·
Yun Zhou · Yi Rong · Ting Zhou · Wenxiang Yang ·
Xiuqing Cui · Weihong Chen**

Abstract The inflammation and fibrosis induced by silica dust are considered to be substantial responses in silicosis progression. Interleukin-1 beta (IL-1β) plays an important role in silica-induced lung inflammation, but the mechanisms that underlie the influence of IL-1β on the progression of silicosis remain unclear. In this study, the role of IL-1β in silica-induced inflammation and fibrosis was evaluated by administering a suspension of 2.5-mg silica dust, either with or without 40 μg anti-mouse IL-1β monoclonal antibody (mAb), to the lungs of male C57BL/6 mice. Silica + anti-IL-1β mAb-treated mice showed the depletion of IL-1β as well as the attenuation of inflammation, as evaluated in the bronchoalveolar lavage fluid (BALF) and histological sections from 1 to 84 days after silica exposure. Further study of the BALF indicated that inhibition of IL-1β could reduce the contents of tumor necrosis factor-alpha and monocyte chemoattractant protein-1. The real-time PCR and pathology results showed that the neutralization of IL-1β attenuated silica-induced fibrosis by inhibiting the gene expression of transforming growth factor-beta 1, collagen I and fibronectin. The examination of Th1-cytokine and Th2-cytokine suggested that depletion of IL-1β decelerated the Th1/Th2 balance toward a Th2-dominant response. In conclusion, the present study suggests that the neutralization of IL-1β attenuates silica-induced inflammation and fibrosis by inhibiting other inflammatory and fibrogenic mediators and modulating the Th1/Th2 balance.

Keywords Silica · IL-1β · Lung inflammation · Lung fibrosis

Introduction

Silicosis and increased mortality have been associated with exposure to crystalline silica, making silica exposure a high-priority public health concern (Barrett et al. 1999; Pernis 2005; Rimal et al. 2005). Silica exposure primarily occurs in workplaces, including metal or coal mining, construction, and glass and clay manufacturing industries (Wilson and Wynn 2009). In addition to occupational exposures, environmental exposure occurs as a result of industrial contaminations, volcanic explosions and sandstorms (Chen et al. 2012). A previous study conducted by Wang et al. (2008) showed that the SiO_2 percentage of sandstorm dust fall in northwest area of China was between 17.36 and 40.09 %.

Silicosis has been studied extensively, yet little is known about the crucial cellular and molecular mechanisms that initiate and propagate the process of inflammation and scarring (Rimal et al. 2005). The pathogenesis of silicosis involves uncontrolled responses of the innate and adaptive immune systems. Cells of the innate immune system, particularly alveolar macrophages, play a fundamental role

J. Guo · N. Gu · Y. Zhou · Y. Rong · T. Zhou · X. Cui ·
W. Chen (✉)
Department of Occupational and Environmental Health and
Ministry of Education Key Lab of Environment and Health,
School of Public Health, Tongji Medical College, Huazhong
University of Science and Technology, Wuhan 430030,
Hubei, China
e-mail: wchen@mails.tjmu.edu.cn

J. Chen
Division of Pneumoconiosis, School of Public Health, China
Medical University, Shenyang 110001, Liaoning, China

T. Shi · W. Yang
Institute of Health Surveillance, Analysis and Protection, Hubei
Center for Disease Control and Prevention, Wuhan 430070,
Hubei, China

in the pathogenesis of silicosis, a condition characterized by lung inflammation and fibrosis (Huaux 2007; Liu et al. 2010). Inhaled silica can be targeted and endocytosed by alveolar macrophages, leading to the release of inflammatory cytokines such as interleukin-1 beta (IL-1β) and tumor necrosis factor-alpha (TNF-α), as well as chemokines like monocyte chemoattractant protein-1 (MCP-1) (Kuroda et al. 2011; Krause et al. 2012; Cho et al. 2007). The silica-induced inflammatory response is initiated and amplified by the burst of inflammatory mediators and the subsequent influx of inflammatory cells. The inflammatory phase is followed by a fibrotic phase in which the extracellular matrix (ECM) is deposited and the tissue is remodeled. It is also known that the activated lung macrophages release fibrogenic cytokines such as transforming growth factor-beta 1 (TGF-β). In addition, other inflammatory cells, such as lymphocytes and neutrophils, amplify the fibrotic responses by producing ECM proteins (Huaux 2007). Finally, adaptive immune polarization (Th1/Th2 response) is thought to be involved in silica-induced fibrosis (Huaux 2007; Pernis 2005).

Many molecular mediators, such as IL-1β, TNF-α, MCP-1 and TGF-β, have been demonstrated to be involved in the development of silicosis (Bai et al. 2010; Mossman and Churg 1998; Hornung et al. 2008). However, the current literature provides little evidence to identify which mediator plays the pivotal role during the silicosis progression. Pathological changes observed in an in vivo study indicated that IL-1β-deficient mice are more resistant to silica-induced inflammation than wild-type mice (Srivastava et al. 2002). Although Piguet's study found that IL-1 receptor antagonist (IL-1Ra) had little or no influence on the silica-induced pulmonary inflammation, this antagonist could suppress and reverse silica-induced pulmonary fibrosis (Piguet et al. 1993). These data suggest that IL-1β exerts a positive function in the silicosis development, but different methods for IL-1β blockade may induce different phenomena. The exact roles of IL-1β in silica-induced pulmonary inflammation and fibrosis therefore need to be clarified (Leung et al. 2012).

In order to address the role of IL-1β in silicosis, we employed an anti-mouse IL-1β monoclonal antibody (mAb) to block the biological function of IL-1β. We did not use gene knockout techniques such as IL-1β knockout or IL-1 receptor (IL-1R) knockout, which is also a good choice to block the biological function of IL-1β, because gene knockout techniques could not be used for clinical treatment at the current stage. Instead, the anti-IL-1β mAb or recombinant IL-1Ra such as anakinra has been proved effective in controlling chronic inflammation in clinical trials (Larsen et al. 2007; Dinarello 2010). At last, the anti-mouse IL-1β mAb was selected for its plasma half-life of one month. This is longer than 4-h half-life of anakinra

(Dinarello 2010), which could not meet the requirement for long-term observation from 1 to 84 days after silica exposure.

The purposes of this study were as follows: (1) to investigate the role of IL-1β in the inflammation and fibrosis phases of the pathogenesis of silicosis and (2) to determine the mechanisms by which IL-1β affects silica-induced inflammation and fibrosis in a mouse model. We used the anti-IL-1β mAb to directly neutralize the silica-induced IL-1β in pulmonary alveoli. We then evaluated the pathologic changes; the gene expression levels of TGF-β, collagen I and fibronectin in the lungs; the cytological alterations; and the concentrations of TNF-α, MCP-1, interferon-gamma (IFN-γ) and interleukin-4 (IL-4) in the bronchoalveolar lavage fluid (BALF). We demonstrated that the neutralization of IL-1β attenuated silica-induced lung inflammation and fibrosis by inhibiting the expression and release of other inflammatory and fibrogenic mediators and by modulating the Th1/Th2 balance.

Methods

Animals

Male C57BL/6 mice (weighing 16–18 g) were purchased from the Center for Animal Experiments, Wuhan University (Wuhan, China). The mice were housed in a specific pathogen-free environment in the Hubei Research Center of Laboratory Animals (Wuhan, China), which is registered with the Provincial Department of Science and Technology, license number of SYXK(E) 2008-0014-00022114. All of the experimental protocols were reviewed and approved by the Animal Care and Use Committee of Tongji Medical College, Huazhong University of Science and Technology, under permit number S301. The animals were acclimated to the environment for 1 week prior to treatment.

Silica preparation

Silica dust (standard α-quartz) (Jia et al. 2011; Shen et al. 2006) was provided by the National Institute of Occupational Health and Poisons Control, Chinese Centers for Disease Control and Prevention (Beijing, China). The percentage of free SiO_2 was greater than 97 %, and the particle diameter was less than 5 μm (diameter <1 μm: 57 %, 1–2 μm: 34 %, 2–3 μm: 4.5 %, 3–4 μm: 3.0 %, 4–5 μm: 1.5 %). After being weighed, the silica dust was sterilized at 121 °C for 20 min and dried. For the intratracheal administration of the silica, the dried silica was suspended in phosphate-buffered saline (PBS) and then sonicated for 10 min (220 V, 50 HZ, SK8200H; Ultrasonic Instrument Co Ltd, Shanghai, China).

Experimental groups and exposure protocol

A total of 128 mice were randomly divided into four groups ($n = 32$ in each group). The groups were as follows: (1) the silica + anti-IL-1β mAb group, in which mice received 2.5-mg silica dust, 10 µl PBS and 40 µl (1 µg/µl) anti-IL-1β mAb (B122) (BioLegend, 11080 Roselle Street, San Diego, CA 92121); (2) the silica + IgG group, in which mice received 2.5-mg silica dust, 10 µl PBS and 40 µl (1 µg/µl) IgG (HTK888) (BioLegend, 11080 Roselle Street, San Diego, CA 92121); (3) the PBS + IgG group, in which mice received 10 µl PBS and 40 µl (1 µg/µl) IgG; and (4) the blank control group, in which mice were untreated.

The silica suspension was administered to mice as described previously (Wang et al. 2010). Briefly, the mice were anesthetized by intraperitoneal injection of 1 % pentobarbital sodium at 45 mg/kg body weight. The trachea was then exposed by an incision of the neck skin and blunt dissection. The suspension was delivered in a final volume of 50 µl by intratracheal administration using a blunted 7-gauge needle. After the treatment was administered, the neck skin was sutured and cleaned with ethanol.

BALF collection and cell counts

At 1, 7, 28 and 84 days after treatment, 8 mice in each group were killed and the lungs were gently lavaged by infusing them with 1 ml cold PBS 3 times. The BALF aliquots were transferred into three sterilized tubes, followed by centrifugation at 1,000 rpm for 10 min at 4 °C. The supernatant of the first tube was separated and stored at −80 °C for later analysis. The pellets of all tubes were washed with PBS and then resuspended in 500 µl PBS for total cell and differential cell counting. A hemocytometer was used to quantify the total cells. For the differential cell counts, smears of each suspension were stained with Wright-Giemsa kits (Nanjing Jiancheng Bioengineering Institute, Nanjing, China), and 300 cells were categorized as macrophages, neutrophils or lymphocytes using standard morphologic criteria.

Analysis of IL-1β, TNF-α, MCP-1, IFN-γ and IL-4 in BALF

The levels of IL-1β, TNF-α, MCP-1, IFN-γ and IL-4 in BALF were measured using enzyme-linked immunosorbent assay (ELISA) kits (Dakewe Biotech Company Limited, Shenzhen, China) according to the manufacturer's instructions. Briefly, a total volume of 150 µl of fluid, which contained 50 µl BALF, 50 µl diluent buffer and 50 µl diluted biotinylated antibody, were added to the wells of the assay plate. The plate was incubated for 90 min at 37 °C, followed by four washes with diluted wash buffer.

Streptavidin-HRP (100 µl/well) was added, and the plate was incubated for another 30 min at 37 °C. After washing the plate again, 100 µl of TMB solution was added to each well, and the plate was incubated in dark for 15 min at 37 °C. Finally, 100 µl of the stop solution was added to each well to stop the reaction. The absorbance values of the wells at 450 nm and 620 nm were obtained. The ELISA was performed in duplicate for every sample.

Analysis of TGF-β, collagen I and fibronectin gene expression in the lung tissues

Quantitative real-time PCR was performed to measure the levels of TGF-β, collagen I and fibronectin mRNA in the right lungs. Total RNA was extracted with Trizol reagent (Invitrogen, Carlsbad, CA, USA) as recommended by the supplier. The RNA concentration was estimated by ultraviolet absorbance at 260 nm, and the RNA purity was tested with an ND1000 spectrophotometer (Thermo Fisher NanoDrop, USA), which showed an optical density ratio (OD260/OD280) of 1.8–2.0. First-strand complementary DNA was synthesized from 2 µg of total RNA by the ReverTra Ace® qPCR RT Kit (FSQ-101, TOYOBO, Japan) according to the manufacturer's recommendations. Quantitative PCR was run on an ABI PRISM® 7900HT Sequence Detection System (Applied Biosystems, USA) using the SYBR® Green Realtime PCR Master Mix (QPK-201, TOYOBO, Japan) according to the manufacturer's instructions. GAPDH was used as an internal control for each run. The primer sequences were as follows: TGF-β, sense 5′-GTGTGGAGCAACATGTGGAACTCTA-3′, anti-sense 5′-CGCTGAATCGAAAGCCCTGTA-3′; collagen I, sense 5′-CTGGCGGTTCAGGTCCAAT-3′, anti-sense 5′-TTCCAGGCAATCCACGAGC-3′; fibronectin, sense 5′-CTATCTATGCTGTGGAGGAG-3′, anti-sense 5′-GAGTTTGGTGGTCTGTTGTG-3′; and GAPDH, sense 5′-AAATGGTGAAGGTCGGTGTGAAC-3′, anti-sense 5′-CAACAATCTCCACTTTGCCACTG-3′. The PCR amplifications were conducted with the following cycling program: 95 °C for 1 min; 40 cycles at 95 °C for 15 s, and 60 °C for 1 min. Real-time PCR reactions were performed in triplicate for each sample. The relative expression of the target genes was calculated using the $2^{-\Delta\Delta Ct}$ method.

Pathological examination

After fixation in paraformaldehyde, the left lungs were embedded in paraffin and sectioned at 5 µm thickness. The sections were stained with hematoxylin and eosin (H&E) and Masson for the pathological evaluation of inflammation and fibrosis, respectively. The micrographs that shown represent the average level of inflammation or fibrosis for each group at each time point.

The lung inflammation was graded into 4 stages and scored as follows (Szapiel et al. 1979): normal lung, scored 0 point; light inflammation, minimal inflammatory thickening of alveolar walls, limited in local area, <20 % of lung area involved, the alveolar structure was normal, scored 1 point; medium inflammation, the inflammation area reached 20–50 % of the whole lung area, scored 2 points; heavy inflammation, lesion involving >50 % of the lung, severe distortion of structure, monocytes infiltration into the alveolar space, consolidation was placed, scored 3 points. The lung fibrosis was graded and scored by Ashcroft's method (Ashcroft et al. 1988): normal lung, scored 0 point; light fibrosis, minimal fibrous thickening of alveolar or bronchiolar walls without obvious damage to lung architecture, scored 1 point; medium fibrosis, moderate thickening of alveolar or bronchiolar walls, damage to alveolar structure and fibrous bands or small fibrous masses, scored 2 points; heavy fibrosis, increased fibrosis with obvious damage to lung structure, consolidation or large fibrous masses, scored 3 points.

Statistical analysis

The results were expressed as the mean ± SEM. Significant differences among the groups were evaluated using one-way analysis of variance (ANOVA) followed by the *Dunnett t test*. For all comparisons, statistical significance was accepted when $P < 0.05$. All analyses were performed using SAS version 9.1 (SAS Institute, Cary, NC, USA).

Results

The time course of changes in IL-1β in BALF and the neutralization efficacy of anti-IL-1β mAb

The time course of changes of IL-1β in BALF are presented in Fig. 1. The BALF concentrations of IL-1β for the silica + IgG group were significantly higher than those in the PBS + IgG or blank control group at all post-exposure time points. Furthermore, the BALF concentrations of IL-1β on days 7, 28 and 84 were significantly higher than that on day 1, but there were no significant differences between day 28 and day 84.

The level of IL-1β in the silica + anti-IL-1β mAb group was 10.5 pg/ml on day 1, similar to the levels in the control mice. The IL-1β levels in the BALF of the silica + anti-IL-1β mAb group gradually increased at the later time points. However, the level of this cytokine remained significantly lower than that in the silica + IgG group through day 84 (Fig. 1). These results indicated that the IL-1β was blocked.
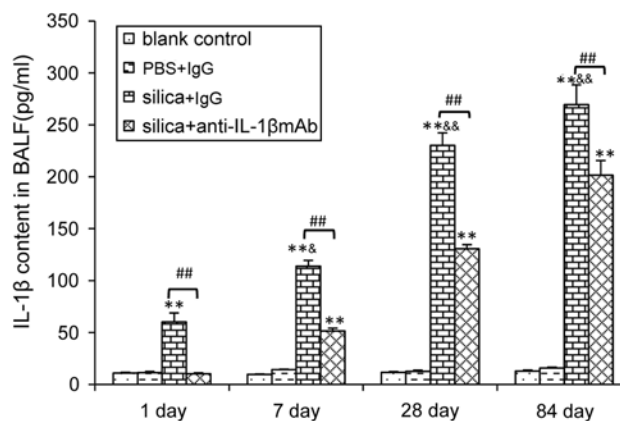

Fig. 1 The time course of changes of IL-1β in BALF and the neutralization efficacy of anti-IL-1β mAb. The concentrations of IL-1β in BALF were assayed by ELISA. Determinations were performed in duplicate and expressed as the mean ± SEM ($n = 6$). Significant differences among the groups were evaluated using a one-way analysis of variance followed by the *Dunnett t test*. **$P < 0.01$ compared with the blank control group at the same time point. &$P < 0.05$ compared with the value at day 1 in the same group. &&$P < 0.01$ compared with the value at day 1 in the same group. ##$P < 0.01$ compared with the silica + IgG group at the same time point

Neutralization of IL-1β attenuated silica-induced pulmonary inflammation

Neutralization of IL-1β attenuated silica-induced inflammatory histopathology changes

There were no indications of inflammation in the lung tissues of the PBS + IgG or blank control group at any of the post-exposure time points (Fig. 2a, b). In the silica + IgG group, a large inflammatory cell infiltration and alveolar septal thickening were observed on day 1 (Fig. 2c1). Lower levels of inflammatory cells and alveolar septal thickening were observed in the silica + anti-IL-1β mAb group on day 1 (Fig. 2d1). Similarly, on day 7, a larger inflammatory cell infiltrate and a more substantial disruption of the alveolar structure were observed in the silica + IgG group compared with the pathology of the silica + anti-IL-1β mAb group (Fig. 2c7, d7). On day 28, the inflammation in the silica + IgG group was further increased relative to the level on day 7 (Fig. 2c28). However, at this time, the inflammation in the silica + anti-IL-1β mAb group was attenuated, and the number of inflammatory cells was reduced relative to those observed on day 7 (Fig. 2d28). Exudates in the alveolar cavity of the silica + IgG group were more abundant than that in the silica + anti-IL-1β mAb group on day 28. On day 84 after silica exposure, the inflammatory responses in the lung tissues had decreased (Fig. 2c84, d84). In brief, as shown in Fig. 2e, the silica-induced inflammatory response in lung tissues was
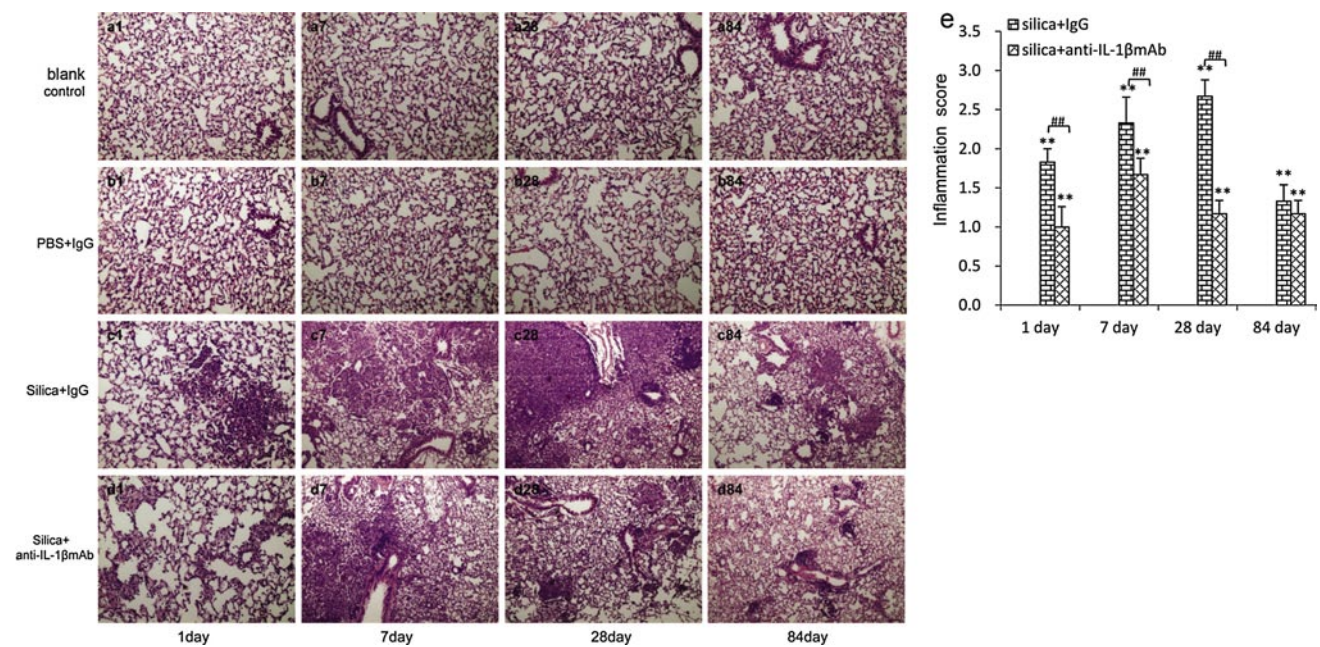
Fig. 2 Neutralization of IL-1β attenuated silica-induced pathologic changes of inflammation (H&E staining, ×200). **a**₁, ₇, ₂₈, ₈₄: Blank control groups; **b**₁, ₇, ₂₈, ₈₄: PBS + IgG groups; **c**₁, ₇, ₂₈, ₈₄: Silica + IgG groups; **d**₁, ₇, ₂₈, ₈₄: Silica + anti-IL-1β mAb groups. a1–d1: day 1; a7–d7: day 7; a28–d28: day 28; a84–d84: day 84. **e**: Inflammation scores of the silica + IgG and silica + anti-IL-1β mAb groups. Values are shown as the mean ± SEM ($n = 6$). Significant differences among the groups were evaluated using a one-way analysis of variance followed by the *Dunnett t test*. **$P < 0.01$ compared with the blank control group at the same time point. ##$P < 0.01$ compared with the silica + IgG group at the same time point

significantly decreased by the usage of anti-IL-1β mAb on days 1, 7 and 28. The neutralization of IL-1β could restrain pulmonary inflammation induced by silica exposure.

Neutralization of IL-1β decreased the total cells and inflammatory cells in BALF

The number of total cells, macrophages, neutrophils and lymphocytes in BALF are shown in Fig. 3. In comparison with the blank control or PBS + IgG group, the number of total cells, macrophages, neutrophils and lymphocytes in both the silica + IgG and silica + anti-IL-1β mAb groups were significantly increased on days 1, 7, 28 and 84 (Fig. 3a–d). However, the number of macrophages and lymphocytes in the silica + anti-IL-1β mAb group was significantly lower compared with the number of these cells in the silica + IgG group at all post-exposure time points (Fig. 3b, d). Furthermore, the number of neutrophils in the silica + anti-IL-1β mAb group was lower when compared with that in the silica + IgG group at days 7 and 28 (Fig. 3c).

Neutralization of IL-1β reduced the silica-induced release of TNF-α and MCP-1 in BALF

Our data showed that the concentrations of TNF-α in the silica + IgG and silica + anti-IL-1β mAb groups were greater than those of the controls (Fig. 4a). The TNF-α levels in the silica + IgG and silica + anti-IL-1β mAb groups increased gradually from day 1, peaking on day 28 after silica exposure. IL-1β antibody treatment significantly reduced the TNF-α levels on days 7, 28 and 84 compared with these levels in silica + IgG-treated mice.

The levels of MCP-1 were significantly increased in the silica + IgG and silica + anti-IL-1β mAb groups relative to the blank control or PBS + IgG group (Fig. 4b). We also observed a similar time course for changes in MCP-1 concentration in the silica + IgG and silica + anti-IL-1β mAb groups. Specifically, the MCP-1 concentrations in these two groups at day 7 were much higher than those at the other post-exposure time points. However, the IL-1β antibody treatment significantly decreased the MCP-1 levels on days 1 and 7.

Neutralization of IL-1β attenuated pulmonary fibrosis after silica exposure

Neutralization of IL-1β attenuated the silica-induced fibrosis in the lung tissue sections

No indications of fibrosis were observed in any group 1 day after treatment (not shown). In addition, no fibrosis was observed in the blank control or PBS + IgG group (Fig. 5a,

Fig. 3 Neutralization of IL-1β decreased the total and inflammatory cell numbers in BALF. The total cell numbers (**a**), macrophage numbers (**b**), neutrophil numbers (**c**) and lymphocyte numbers (**d**) were evaluated by Wright-Giemsa staining. Values are shown as the mean ± SEM (*n* = 6). Significant differences among the groups were evaluated using a one-way analysis of variance followed by the *Dunnett t test*. **$P < 0.01$ compared with the blank control group at the same time point. #$P < 0.05$ compared with the silica + IgG group at the same time point. ##$P < 0.01$ compared with the silica + IgG group at the same time point
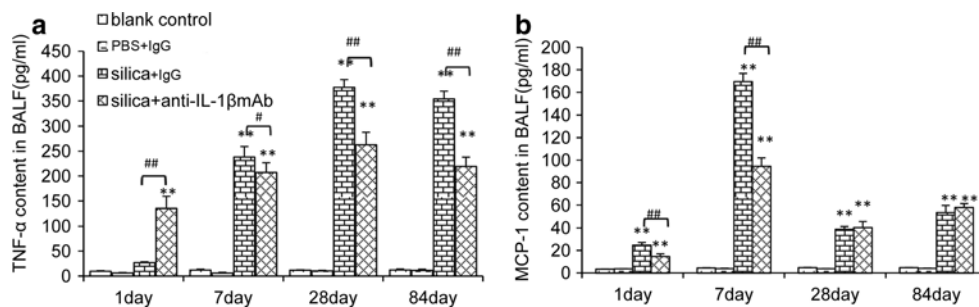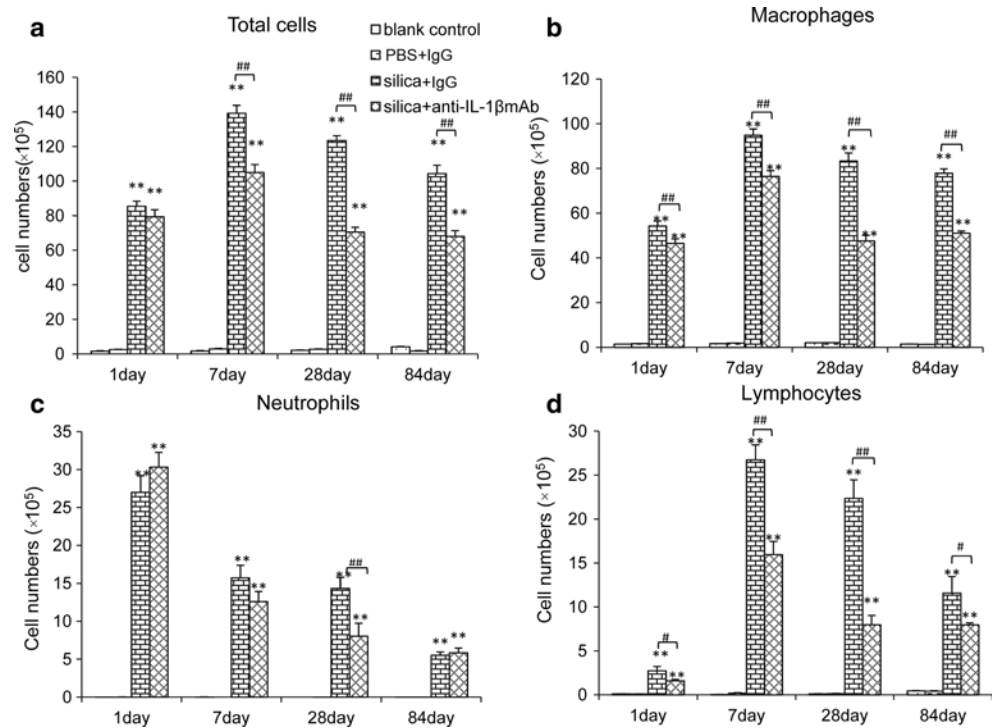

Fig. 4 Neutralization of IL-1β reduced the silica-induced release of TNF-α and MCP-1 in BALF. The concentrations of TNF-α (**a**) and MCP-1 (**b**) were measured by ELISA. Determinations were performed in duplicate and represented as the mean ± SEM (*n* = 6). Significant differences among the groups were evaluated using a one-way analysis of variance followed by the *Dunnett t test*. **$P < 0.01$ compared with the blank control group at the same time point. #$P < 0.05$ compared with the silica + IgG group at the same time point. ##$P < 0.01$ compared with the silica + IgG group at the same time point

b). In the silica + IgG group, minimal fibrotic thickening of the bronchiolar walls was occasionally observed on day 7 (Fig. 5c7). In the silica + anti-IL-1β mAb group, rare fibrotic changes were observed on day 7 (Fig. 5d7). On day 28, after silica + IgG exposure, collagen deposition and fibrous bands or small fibrous masses were observed, the alveolar structures were damaged and small areas of consolidation had formed (Fig. 5c28). Collagen deposition in the silica + anti-IL-1β mAb group was less than that in the silica + IgG group (Fig. 5d28). Larger areas of fibrous bands or fibrous masses were observed in the silica + IgG group (Fig. 5c84) than those in the silica + anti-IL-1β mAb group (Fig. 5d84) through day 84. When using fibrosis

score to quantify the fibrotic changes, the results suggested that blocking IL-1β at the beginning of silica exposure could significantly attenuate the silica-induced fibrosis on days 7, 28 and 84 (Fig. 5e).

Neutralization of IL-1β inhibited the expression of TGF-β, collagen I and fibronectin in the lung tissue

As shown in Fig. 6a and c, the mRNA levels of TGF-β and fibronectin in the silica + IgG and silica + anti-IL-1β mAb groups were obviously higher than those in the PBS + IgG group on days 28 and 84. IL-1β antibody treatment caused a statistically significant decrease in the TGF-β and
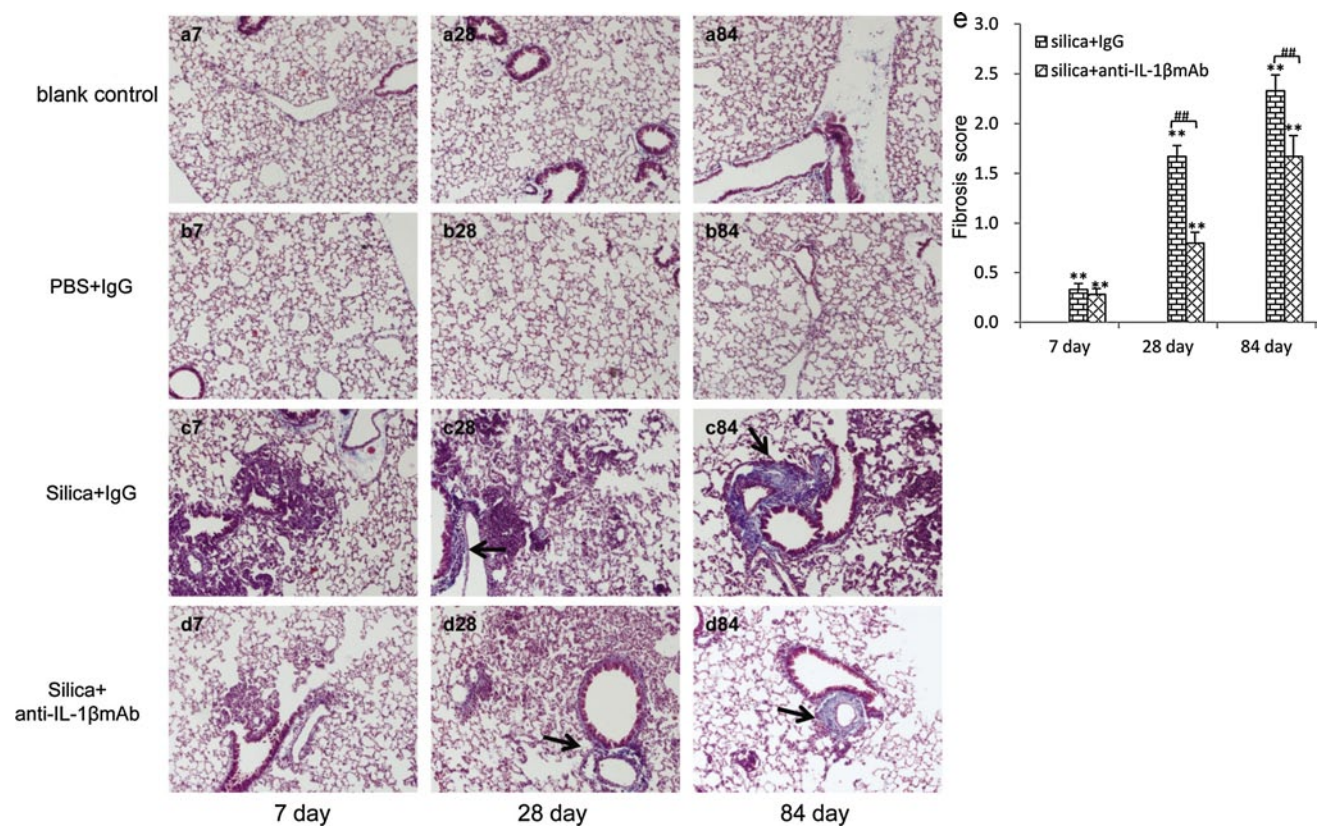
Fig. 5 Neutralization of IL-1β attenuated the silica-induced fibrosis in the lung tissue sections (Masson staining, ×200). **a**$_{7, 28, 84}$: Blank control groups; **b**$_{7, 28, 84}$: PBS + IgG groups; **c**$_{7, 28, 84}$: Silica + IgG groups; **d**$_{7, 28, 84}$: Silica + anti-IL-1β mAb groups. a7–d7: day 7; a28–d28: day 28; a84–d84: day 84. **e**: Fibrosis scores of the silica + IgG and silica + anti-IL-1β mAb groups. The arrows denoted the collagen deposition. Values are shown as the mean ± SEM ($n = 6$). Significant differences among the groups were evaluated using a one-way analysis of variance followed by the *Dunnett t test*. **$P < 0.01$ compared with the blank control group at the same time point. ##$P < 0.01$ compared with the silica + IgG group at the same time point

fibronectin mRNA levels on days 28 and 84. The level of collagen I mRNA in the silica + IgG and silica + anti-IL-1β mAb groups was significantly higher than that in the PBS + IgG group on day 7. In comparison with those in the silica + IgG group, the level of collagen I mRNA was significantly decreased in the silica + anti-IL-1β mAb group at 7, 28 and 84 days after treatment (Fig. 6b).

Neutralization of IL-1β changed the Th1/Th2 balance in the lung

The concentrations of IFN-γ and IL-4 in the silica + IgG and silica + anti-IL-1β mAb groups were significantly increased at 7, 28 and 84 days after silica exposure. However, the IL-1β antibody treatment increased the levels of IFN-γ and decreased the levels of IL-4 at all the three post-exposure time points relative to the silica + IgG treatment (Fig. 7a, b). To further clarify the Th1/Th2 balance, we used the ratio of IFN-γ/IL-4 to represent the Th1/Th2 balance (Fig. 7c, d). The results showed that the ratios of IFN-γ/IL-4 in the silica + IgG and silica + anti-IL-1β mAb groups were significantly decreased relative to those in the control mice, but the ratio in the silica + anti-IL-1β mAb group was significantly higher than that in the silica + IgG group on days 7, 28 and 84 after treatment.

Discussion

In this study, we provided insight into the role of IL-1β in the progression of silicosis in a mouse model by neutralizing silica-induced IL-1β with an anti-mouse IL-1β mAb. Although silica-induced IL-1β could not be completely neutralized by the intratracheal administration of anti-IL-1β mAb, the effect of neutralization was maintained through day 84 after silica exposure. Our results suggest that IL-1β plays a key role in elevating TNF-α and MCP-1 levels; increasing TGF-β, collagen I and fibronectin gene expression; and modulating the Th1/Th2 balance after the exposure of the lungs to silica.
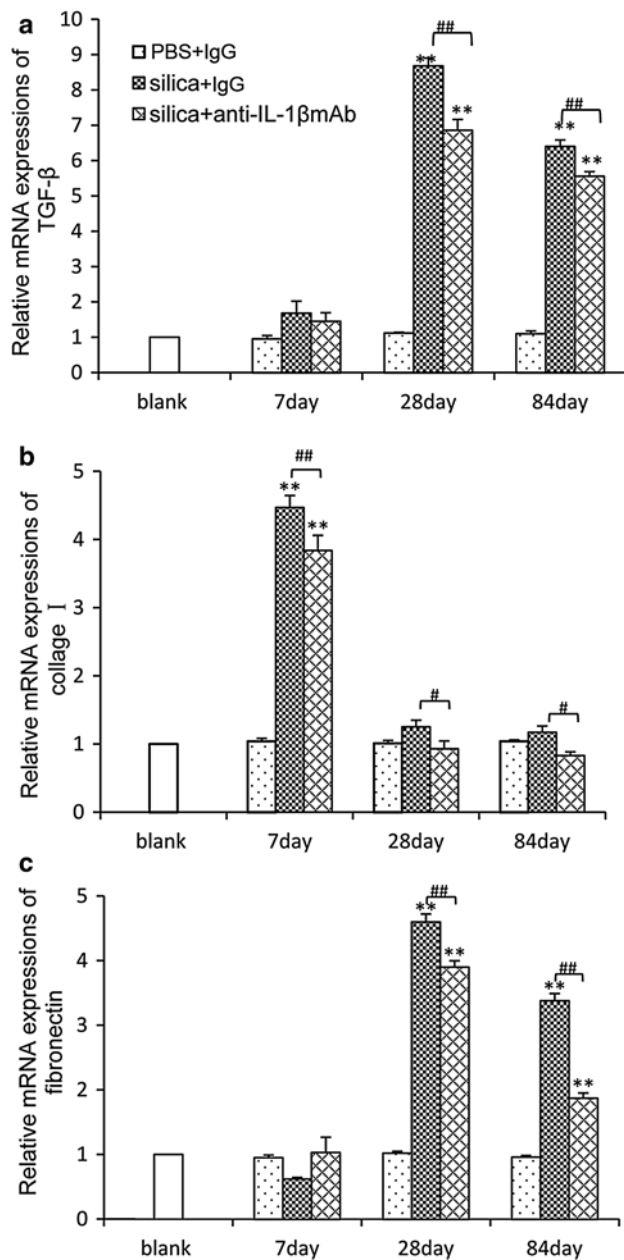
Fig. 6 Neutralization of IL-1β reduced the expression of TGF-β, collagen I, and fibronectin genes in the lung tissue. The relative mRNA expressions of TGF-β (**a**), collagen I (**b**) and fibronectin (**c**) were determined by RT-PCR. The housekeeping gene GAPDH was used as an internal control. The relative expression of target genes were calculated using $2^{-\Delta\Delta Ct}$. Values are shown as the mean ± SEM ($n = 6$). Significant differences among the groups were evaluated using a one-way analysis of variance followed by the *Dunnett t test*. **$P < 0.01$ compared with the PBS + IgG group at the same time point. #$P < 0.05$ compared with the silica + IgG group at the same time point. ##$P < 0.01$ compared with the silica + IgG group at the same time point

The IL-1β level of the silica + IgG group remained elevated in the BALF compared with those in the blank or PBS + IgG control groups at all post-exposure time points

(days 1, 7, 28 and 84) in this study (Fig. 1). Similar phenomenon was also reported by Song' study. They observed persistently high gene expression of IL-1β after silica exposure (Song et al. 2012). Inhaled silica particles are first engulfed by the alveolar macrophages. Recent evidences suggest that silica particles are capable of activating the Nalp3 inflammasome, which could cleave the inactive pro-IL-1β precursor to the mature IL-1β in the macrophages. On this basis, more mature IL-1β was released directly by the macrophages (Dostert et al. 2008; Cassel et al. 2008). Meanwhile, the toxicity of the silica then causes either macrophage membrane damage or macrophage death. Then some inflammatory mediators, including enzymes and cytokines together with intracellular silica, are released into the alveolar space. The released intracellular silica particles are then taken up by other macrophages (Rimal et al. 2005). This recurring cycle of alveolar macrophage phagocytosis and cell rupture perpetuates and expands the chronic inflammation induced by silica and may be an important mechanism for the persistently high expression of the IL-1β in the BALF after silica exposure. Our results support that IL-1β exerts a persistent function in the microenvironment of chronic inflammation in the progression of silicosis.

According to our results of differential cell count, the decreased lymphocytes count of the silica + anti-IL-1β mAb group suggests that anti-IL-1β mAb may inhibit the silica-induced influx of lymphocytes (Fig. 3d), cells of the adaptive immune system. The role of lymphocytes in silica-induced inflammation is still in debate at present. Previous studies in vitro have reported that silica exposure had no effects on T lymphocytes (Hubbard 1989). However, some studies of mouse silicosis model showed that silica significantly elevated the number of lymphocytes in the BALF (Song et al. 2012; Liu et al. 2010), which are consistent with our results. Beamer and his colleagues further indicated that lymphocytes could participate in the regulation of silica-induced inflammation through modulation of the Nalp3 inflammasome (Beamer et al. 2010). The activation of the adaptive immune system is a consequence of the activation of the cells of the innate immune system, such as macrophages, and the stimulation of some cells in the adaptive immune system, which could connect the innate and adaptive immune systems (Pernis 2005; Eisenbarth and Flavell 2009; Peng et al. 2007; Beamer et al. 2010). Our results suggest that IL-1β and lymphocytes might be important mediators connecting the innate and adaptive immune systems during silicosis development.

Our study showed that the elevated levels of TNF-α after silica exposure were significantly inhibited by anti-IL-1β mAb, especially on days 7, 28 and 84 (Fig. 4a). A previous study in a mouse silicosis model demonstrated that both IL-1β and TNF-α were associated with silica-induced

Fig. 7 Neutralization of IL-1β affected the Th1/Th2 balance in the lung. The concentrations of IFN-γ (**a**) and IL-4 (**b**) were measured by ELISA. The ratio of IFN-γ/IL-4 concentrations (**c**, **d**) was calculated. Analyses were performed in duplicate and presented as the mean ± SEM ($n = 6$). The significant differences among the groups were evaluated using a one-way analysis of variance followed by the *Dunnett t test*. *$P < 0.05$ compared with the blank control group at the same time point. **$P < 0.01$ compared with the blank control group at the same time point. #$P < 0.05$ compared with the silica + IgG group at the same time point. ##$P < 0.01$ compared with the silica + IgG group at the same time point
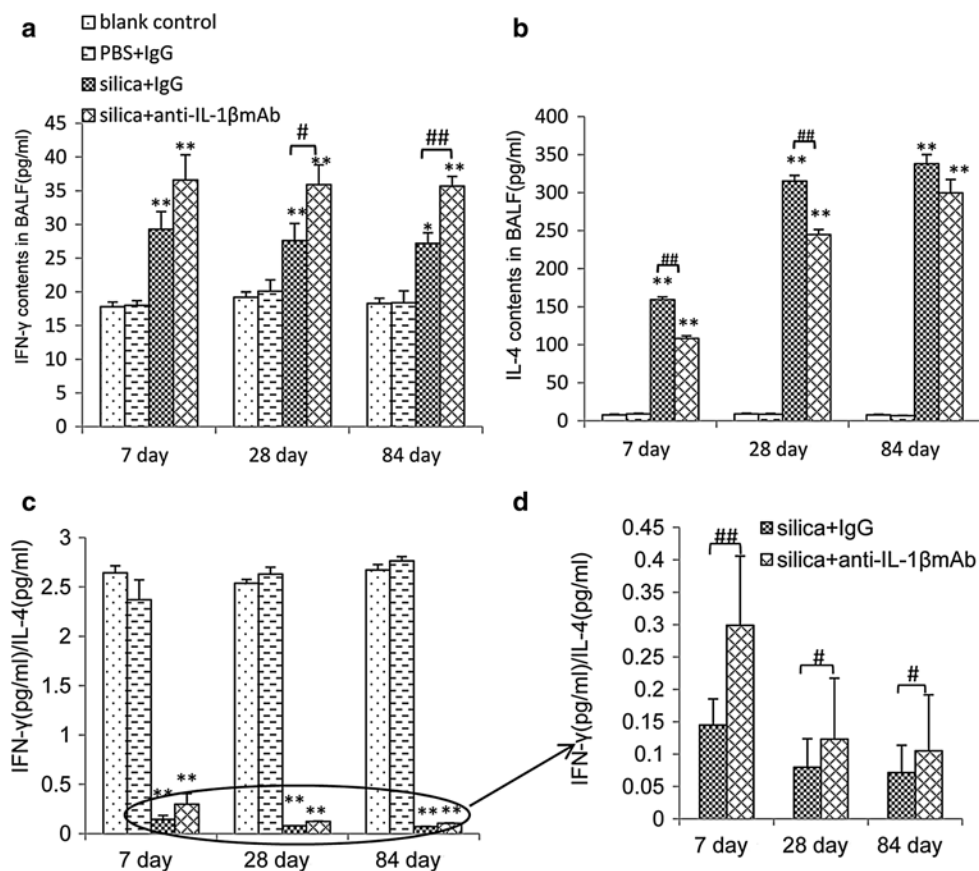
inflammation (Davis et al. 1998). Cardell and his colleagues observed that the co-culture of whole murine tracheas and recombinant murine IL-1β resulted in enhanced pulmonary inflammation through the induction of TNF-α (Cardell et al. 2008). The study conducted by Cassel and his colleagues showed that the silica-induced IL-1β secretion was earlier than that of TNF-α (Cassel et al. 2008). We found that neutralization of IL-1β directly suppressed the expression of TNF-α in this silicosis model. All of these results are consistent with the hypothesis that IL-1β and TNF-α are important cytokines in silicosis development and that TNF-α might be modulated by IL-1β.

Interestingly, the TNF-α levels of the silica + anti-IL-1β mAb-treated mice were higher than those of the mice in the silica + IgG group on day 1 (Fig. 4a). It indicated that TNF-α could not be significantly suppressed by anti-IL-1β mAb right after silica exposure. There are two possible reasons for this phenomenon. Firstly, in our animal model, anti-IL-1β could induce a transient but substantial deficiency of IL-1β, which was necessary for the maintenance of inflammation. Both IL-1β and TNF-α have been identified as pro-inflammatory cytokines (Rimal et al. 2005). We conjecture that the higher TNF-α could be attributed to a compensatory response to the loss of IL-1β to maintain the silica-induced acute inflammatory response.

Secondly, TNF-α might also be induced through other routes, and the inhibitive effect of anti-IL-1β on TNF-α was not exerted within a very short period of time after silica exposure. Moreover, we noted that the increased TNF-α in silica + anti-IL-1β mAb group on day 1 did not appear to disturb the effects of anti-IL-1β on attenuating the silica-induced chronic inflammation and fibrosis in our study.

The time course of the changes in MCP-1 were not consistent with those of IL-1β and TNF-α in the BALF of the silica-exposed groups (Figs. 1, 4). The levels of MCP-1 decreased on day 28 after silica exposure, whereas the levels of IL-1β and TNF-α continued to increase until day 28 after silica exposure. The decreased levels of MCP-1 may suggest that MCP-1 functions primarily in acute inflammation after silica exposure, whereas the persistent inflammation might be regulated by the IL-1β and TNF-α levels. Otherwise, our study found that anti-IL-1β mAb could inhibit the production of MCP-1 at days 1 and 7 after silica exposure (Fig. 4b). Previous research found that MCP-1 played a role in the activation and migration of leukocytes during the inflammatory response (Jiang et al. 1992; Cho et al. 2007; Tanaka et al. 2000; Rao et al. 2004). These results indicated that IL-1β might induce infiltration of the inflammatory cells by stimulating the expression of MCP-1.

Our study also investigated the role of IL-1β in silica-induced fibrosis. The pathology results indicated that anti-IL-1β mAb could attenuate the silica-induced collagen deposition (Fig. 5), consistent with the previous study of Cassel in which Nalp3-deficient mice showed less collagen deposition compared with normal mice after silica exposure (Cassel et al. 2008). Furthermore, Piguet et al. found that IL-1Ra could reduce and reverse silica-induced fibrosis, which was also supported our results (Piguet et al. 1993). We then measured the gene expression levels of TGF-β, collagen I and fibronectin and found that the expression of the TGF-β, collagen I and fibronectin gene was suppressed by the anti-IL-1β mAb, particularly on days 28 and 84 after silica exposure (Fig. 6). TGF-β is an important cytokine involved in the differentiation of fibroblasts into myofibroblasts, which produce components essential to the ECM, such as collagen I and fibronectin (Wynn 2008). Arribillaga et al. reported that an inhibitor of TGF-β could downregulate the expression of collagen I and fibronectin (Arribillaga et al. 2011). These results suggest that IL-1β contributes to the promotion of silica-induced fibrosis by increasing the expression of TGF-β.

In addition to the modulation of TGF-β, we found that an IL-1β-induced alteration in the Th1/Th2 balance may be a contributing mechanism to silica-induced fibrosis. Although the Th1/Th2 balance during the development of silica-induced lung fibrosis is still a matter of debate, it is accepted that both the Th1 and Th2 immune responses are necessary for silicosis (Huaux 2007). Previous studies indicated that the Th2 immune responses are primarily involved in the fibrotic stage after silica exposure (Barbarin et al. 2005; Chen et al. 2005). In our study, we assayed representative Th1 (IFN-γ) and Th2 (IL-4) cytokines in the BALF by ELISA (Fig. 7). We found that silica exposure induced a switch from the Th1 to the Th2 immune response, consistent with the results of a previous study (Liu et al. 2010). The neutralization of IL-1β partially suppressed the Th1 to Th2 switch, suggesting that IL-1β may play a positive role in the modulation of the Th1/Th2 balance toward a Th2-dominant response during the development of silicosis.

In conclusion, our findings demonstrate that the neutralization of IL-1β attenuates silica-induced lung inflammation and fibrosis. Specifically, the neutralization of IL-1β may limit silica-induced inflammation by suppressing other inflammatory mediators and may attenuate silica-induced fibrosis by modulating the TGF-β levels and the Th1/Th2 balance. It is suggested that IL-1β is an attractive target for potential therapeutic intervention of silicosis, and anti-IL-1β antibody has the potential in the prevention of silicosis.

References

Arribillaga L, Dotor J, Basagoiti M, Riezu-Boj JI, Borras-Cuesta F, Lasarte JJ, Sarobe P, Cornet ME, Feijoo E (2011) Therapeutic effect of a peptide inhibitor of TGF-beta on pulmonary fibrosis. Cytokine 53:327–333

Ashcroft T, Simpson JM, Timbrell V (1988) Simple method of estimating severity of pulmonary fibrosis on a numerical scale. J Clin Pathol 41:467–470

Bai R, Zhang L, Liu Y, Meng L, Wang L, Wu Y, Li W, Ge C, Le Guyader L, Chen C (2010) Pulmonary responses to printer toner particles in mice after intratracheal instillation. Toxicol Lett 199:288–300

Barbarin V, Xing Z, Delos M, Lison D, Huaux F (2005) Pulmonary overexpression of IL-10 augments lung fibrosis and Th2 responses induced by silica particles. Am J Physiol Lung Cell Mol Physiol 288:L841–L848

Barrett EG, Johnston C, Oberdorster G, Finkelstein JN (1999) Silica-induced chemokine expression in alveolar type II cells is mediated by TNF-alpha-induced oxidant stress. Am J Physiol 276:L979–L988

Beamer CA, Migliaccio CT, Jessop F, Trapkus M, Yuan D, Holian A (2010) Innate immune processes are sufficient for driving silicosis in mice. J Leukoc Biol 88:547–557

Cardell LO, Uddman R, Zhang Y, Adner M (2008) Interleukin-1beta up-regulates tumor necrosis factor receptors in the mouse airways. Pulm Pharmacol Ther 21:675–681

Cassel SL, Eisenbarth SC, Iyer SS, Sadler JJ, Colegio OR, Tephly LA, Carter AB, Rothman PB, Flavell RA, Sutterwala FS (2008) The Nalp3 inflammasome is essential for the development of silicosis. Proc Natl Acad Sci USA 105:9035–9040

Chen Y, Chen J, Dong J, Liu W (2005) Antifibrotic effect of interferon gamma in silicosis model of rat. Toxicol Lett 155:353–360

Chen W, Liu Y, Wang H, Hnizdo E, Sun Y, Su L, Zhang X, Weng S, Bochmann F, Hearl FJ, Chen J, Wu T (2012) Long-term exposure to silica dust and risk of total and cause-specific mortality in chinese workers: a cohort study. PLoS Med 9:e1001206

Cho WS, Choi M, Han BS, Cho M, Oh J, Park K, Kim SJ, Kim SH, Jeong J (2007) Inflammatory mediators induced by intratracheal instillation of ultrafine amorphous silica particles. Toxicol Lett 175:24–33

Davis GS, Pfeiffer LM, Hemenway DR (1998) Persistent overexpression of interleukin-1beta and tumor necrosis factor-alpha in murine silicosis. J Environ Pathol Toxicol Oncol 17:99–114

Dinarello CA (2010) Why not treat human cancer with interleukin-1 blockade? Cancer Metastasis Rev 29:317–329

Dostert C, Petrilli V, Van Bruggen R, Steele C, Mossman BT, Tschopp J (2008) Innate immune activation through Nalp3 inflammasome sensing of asbestos and silica. Science 320:674–677

Eisenbarth SC, Flavell RA (2009) Innate instruction of adaptive immunity revisited: the inflammasome. EMBO Mol Med 1:92–98

Hornung V, Bauernfeind F, Halle A, Samstad EO, Kono H, Rock KL, Fitzgerald KA, Latz E (2008) Silica crystals and aluminum salts activate the NALP3 inflammasome through phagosomal destabilization. Nat Immunol 9:847–856

Huaux F (2007) New developments in the understanding of immunology in silicosis. Curr Opin Allergy Clin Immunol 7:168–173

Hubbard AK (1989) Role for T lymphocytes in silica-induced pulmonary inflammation. Lab Invest 61:46–52

Jia X, Liu B, Shi X, Ye M, Zhang F, Liu H (2011) Roles of the ERK, JNK/AP-1/cyclin D1-CDK4 pathway in silica-induced cell cycle changes in human embryo lung fibroblast cells. Cell Biol Int 35:697–704

Jiang Y, Beller DI, Frendl G, Graves DT (1992) Monocyte chemoattractant protein-1 regulates adhesion molecule expression and cytokine production in human monocytes. J Immunol 148:2423–2428

Krause K, Metz M, Makris M, Zuberbier T, Maurer M (2012) The role of interleukin-1 in allergy-related disorders. Curr Opin Allergy Clin Immunol 12:477–484

Kuroda E, Ishii KJ, Uematsu S, Ohata K, Coban C, Akira S, Aritake K, Urade Y, Morimoto Y (2011) Silica crystals and aluminum salts regulate the production of prostaglandin in macrophages via NALP3 inflammasome-independent mechanisms. Immunity 34:514–526

Larsen CM, Faulenbach M, Vaag A, Volund A, Ehses JA, Seifert B, Mandrup-Poulsen T, Donath MY (2007) Interleukin-1-receptor antagonist in type 2 diabetes mellitus. N Engl J Med 356:1517–1526

Leung CC, Yu IT, Chen W (2012) Silicosis. Lancet 379:2008–2018

Liu F, Liu J, Weng D, Chen Y, Song L, He Q, Chen J (2010) CD4+ CD25+ Foxp3+ regulatory T cells depletion may attenuate the development of silica-induced lung fibrosis in mice. PLoS One 5:e15404

Mossman BT, Churg A (1998) Mechanisms in the pathogenesis of asbestosis and silicosis. Am J Respir Crit Care Med 157:1666–1680

Peng Y, Martin DA, Kenkel J, Zhang K, Ogden CA, Elkon KB (2007) Innate and adaptive immune response to apoptotic cells. J Autoimmun 29:303–309

Pernis B (2005) Silica and the immune system. Acta Biomed 76(Suppl 2):38–44

Piguet PF, Vesin C, Grau GE, Thompson RC (1993) Interleukin 1 receptor antagonist (IL-1ra) prevents or cures pulmonary fibrosis elicited in mice by bleomycin or silica. Cytokine 5:57–61

Rao KM, Porter DW, Meighan T, Castranova V (2004) The sources of inflammatory mediators in the lung after silica exposure. Environ Health Perspect 112:1679–1686

Rimal B, Greenberg AK, Rom WN (2005) Basic pathogenetic mechanisms in silicosis: current understanding. Curr Opin Pulm Med 11:169–173

Shen F, Fan X, Liu B, Jia X, Du H, You B, Ye M, Huang C, Shi X (2006) Overexpression of cyclin D1-CDK4 in silica-induced transformed cells is due to activation of ERKs, JNKs/AP-1 pathway. Toxicol Lett 160:185–195

Song L, Weng D, Liu F, Chen Y, Li C, Dong L, Tang W, Chen J (2012) Tregs promote the differentiation of th17 cells in silica-induced lung fibrosis in mice. PLoS One 7:e37286

Srivastava KD, Rom WN, Jagirdar J, Yie TA, Gordon T, Tchou-Wong KM (2002) Crucial role of interleukin-1beta and nitric oxide synthase in silica-induced inflammation and apoptosis in mice. Am J Respir Crit Care Med 165:527–533

Szapiel SV, Elson NA, Fulmer JD, Hunninghake GW, Crystal RG (1979) Bleomycin-induced interstitial pulmonary disease in the nude, athymic mouse. Am Rev Respir Dis 120:893–899

Tanaka S, Choe N, Iwagaki A, Hemenway DR, Kagan E (2000) Asbestos exposure induces MCP-1 secretion by pleural mesothelial cells. Exp Lung Res 26:241–255

Wang ZQ, Wang SG, Gao JX, Gao SQ (2008) Characteristic of dust-fall in sandstrom in Northwest Area of China. J Environ Health 25:1053–1055

Wang X, Lv L, Chen Y, Chen J (2010) A CD36 synthetic peptide inhibits silica-induced lung fibrosis in the mice. Toxicol Ind Health 26:47–53

Wilson MS, Wynn TA (2009) Pulmonary fibrosis: pathogenesis, etiology and regulation. Mucosal Immunol 2:103–121

Wynn TA (2008) Cellular and molecular mechanisms of fibrosis. J Pathol 214:199–210